EUROPEAN ORGANIZATION FOR NUCLEAR RESEARCH

CERN–PPE/97–27

7 March 1997

Rapidity Correlations in Λ Baryon and Proton Production in Hadronic Z^0 Decays

DELPHI Collaboration

Abstract

In an analysis of multihadronic events recorded at LEP by DELPHI in the years 1992 through 1994, charged hadrons are identified using the measurement of their energy loss and their Cherenkov angle. Rapidity correlations of Λ-Λ, proton-proton, and Λ-proton pairs are compared. The agreement with the string and cluster fragmentation models is tested. For those pairs that frame a meson in terms of rapidity the compensation of strangeness is studied. For $\Lambda\overline{\mathrm{p}}$ pairs the additional correlation with respect to charged kaons is analysed.

(To be submitted to Zeit. f. Physik C.)

P.Abreu[21], W.Adam[49], T.Adye[36], I.Ajinenko[41], G.D.Alekseev[16], R.Alemany[48], P.P.Allport[22], S.Almehed[24], U.Amaldi[9], S.Amato[46], A.Andreazza[9], M.L.Andrieux[14], P.Antilogus[9], W-D.Apel[17], B.Åsman[43], J-E.Augustin[25], A.Augustinus[30], P.Baillon[9], P.Bambade[19], F.Barao[21], M.Barbi[46], D.Y.Bardin[16], G.Barker[9], A.Baroncelli[39], O.Barring[24], M.J.Bates[36], M.Battaglia[15], M.Baubillier[23], J.Baudot[38], K-H.Becks[51], M.Begalli[6], P.Beilliere[8], Yu.Belokopytov[9,52], K.Belous[41], A.C.Benvenuti[5], M.Berggren[46], D.Bertini[25], D.Bertrand[2], M.Besancon[38], F.Bianchi[44], M.Bigi[44], M.S.Bilenky[16], P.Billoir[23], M-A.Bizouard[19], D.Bloch[10], M.Blume[51], M.Bonesini[27], W.Bonivento[27], P.S.L.Booth[22], A.W.Borgland[4], G.Borisov[38,41], C.Bosio[39], O.Botner[47], E.Boudinov[30], B.Bouquet[19], C.Bourdarios[19], T.J.V.Bowcock[22], I.Bozovic[11], M.Bozzo[13], P.Branchini[39], K.D.Brand[35], T.Brenke[51], R.A.Brenner[47], C.Bricman[2], R.C.A.Brown[9], P.Bruckman[18], J-M.Brunet[8], L.Bugge[32], T.Buran[32], T.Burgsmueller[51], P.Buschmann[51], S.Cabrera[48], M.Caccia[27], M.Calvi[27], A.J.Camacho Rozas[40], T.Camporesi[9], V.Canale[37], M.Canepa[13], K.Cankocak[43], F.Cao[2], F.Carena[9], L.Carroll[22], C.Caso[13], M.V.Castillo Gimenez[48], A.Cattai[9], F.R.Cavallo[5], V.Chabaud[9], Ph.Charpentier[9], L.Chaussard[25], P.Checchia[35], G.A.Chelkov[16], M.Chen[2], R.Chierici[44], P.Chliapnikov[41], P.Chochula[7], V.Chorowicz[25], J.Chudoba[29], V.Cindro[42], P.Collins[9], R.Contri[13], E.Cortina[48], G.Cosme[19], F.Cossutti[45], J-H.Cowell[22], H.B.Crawley[1], D.Crennell[36], G.Crosetti[13], J.Cuevas Maestro[33], S.Czellar[15], J.Dahm[51], B.Dalmagne[19], M.Dam[28], G.Damgaard[28], P.D.Dauncey[36], M.Davenport[9], W.Da Silva[23], A.Deghorain[2], G.Della Ricca[45], P.Delpierre[26], N.Demaria[34], A.De Angelis[9], W.De Boer[17], S.De Brabandere[2], C.De Clercq[2], C.De La Vaissiere[23], B.De Lotto[45], A.De Min[35], L.De Paula[46], H.Dijkstra[9], L.Di Ciaccio[37], A.Di Diodato[37], A.Djannati[8], J.Dolbeau[8], K.Doroba[50], M.Dracos[10], J.Drees[51], K.-A.Drees[51], M.Dris[31], J-D.Durand[25,9], D.Edsall[1], R.Ehret[17], G.Eigen[4], T.Ekelof[47], G.Ekspong[43], M.Elsing[9], J-P.Engel[10], B.Erzen[42], M.Espirito Santo[21], E.Falk[24], G.Fanourakis[11], D.Fassouliotis[45], M.Feindt[9], P.Ferrari[27], A.Ferrer[48], S.Fichet[23], T.A.Filippas[31], A.Firestone[1], P.-A.Fischer[10], H.Foeth[9], E.Fokitis[31], F.Fontanelli[13], F.Formenti[9], B.Franek[36], A.G.Frodesen[4], R.Fruhwirth[49], F.Fulda-Quenzer[19], J.Fuster[48], A.Galloni[22], D.Gamba[44], M.Gandelman[46], C.Garcia[48], J.Garcia[40], C.Gaspar[9], U.Gasparini[35], Ph.Gavillet[9], E.N.Gazis[31], D.Gele[10], J-P.Gerber[10], L.Gerdyukov[41], R.Gokieli[50], B.Golob[42], P.Goncalves[21], G.Gopal[36], L.Gorn[1], M.Gorski[50], Yu.Gouz[44,52], V.Gracco[13], E.Graziani[39], C.Green[22], A.Grefrath[51], P.Gris[38], G.Grosdidier[19], K.Grzelak[50], S.Gumenyuk[41], P.Gunnarsson[43], M.Gunther[47], J.Guy[36], F.Hahn[9], S.Hahn[51], Z.Hajduk[18], A.Hallgren[47], K.Hamacher[51], F.J.Harris[34], V.Hedberg[24], R.Henriques[21], J.J.Hernandez[48], P.Herquet[2], H.Herr[9], T.L.Hessing[34], J.-M.Heuser[51], E.Higon[48], H.J.Hilke[9], S-O.Holmgren[43], P.J.Holt[34], D.Holthuizen[30], S.Hoorelbeke[2], M.Houlden[22], J.Hrubec[49], K.Huet[2], K.Hultqvist[43], J.N.Jackson[22], R.Jacobsson[43], P.Jalocha[18], R.Janik[7], Ch.Jarlskog[24], G.Jarlskog[24], P.Jarry[38], B.Jean-Marie[19], E.K.Johansson[43], L.Jonsson[24], P.Jonsson[24], C.Joram[9], P.Juillot[10], M.Kaiser[17], F.Kapusta[23], K.Karafasoulis[11], M.Karlsson[43], S.Katsanevas[25], E.C.Katsoufis[31], R.Keranen[4], Yu.Khokhlov[41], B.A.Khomenko[16], N.N.Khovanski[16], B.King[22], N.J.Kjaer[30], O.Klapp[51], H.Klein[9], P.Kluit[30], D.Knoblauch[17], B.Koene[30], P.Kokkinias[11], M.Koratzinos[9], K.Korcyl[18], V.Kostioukhine[41], C.Kourkoumelis[3], O.Kouznetsov[13,16], M.Krammer[49], C.Kreuter[9], I.Kronkvist[24], Z.Krumstein[16], W.Krupinski[18], P.Kubinec[7], W.Kucewicz[18], K.Kurvinen[15], C.Lacasta[9], I.Laktineh[25], J.W.Lamsa[1], L.Lanceri[45], D.W.Lane[1], P.Langefeld[51], V.Lapin[41], J-P.Laugier[38], R.Lauhakangas[15], F.Ledroit[14], V.Lefebure[2], C.K.Legan[1], A.Leisos[11], R.Leitner[29], J.Lemonne[2], G.Lenzen[51], V.Lepeltier[19], T.Lesiak[18], J.Libby[34], D.Liko[9], R.Lindner[51], A.Lipniacka[43], I.Lippi[35], B.Loerstad[24], J.G.Loken[34], J.M.Lopez[40], D.Loukas[11], P.Lutz[38], L.Lyons[34], J.MacNaughton[49], G.Maehlum[17], J.R.Mahon[6], A.Maio[21], T.G.M.Malmgren[43], V.Malychev[16], F.Mandl[49], J.Marco[40], R.Marco[40], B.Marechal[46], M.Margoni[35], J-C.Marin[9], C.Mariotti[9], A.Markou[11], C.Martinez-Rivero[33], F.Martinez-Vidal[48], S.Marti i Garcia[22], J.Masik[29], F.Matorras[40], C.Matteuzzi[27], G.Matthiae[37], M.Mazzucato[35], M.Mc Cubbin[22], R.Mc Kay[1], R.Mc Nulty[9], J.Medbo[47], M.Merk[30], C.Meroni[27], S.Meyer[17], W.T.Meyer[1], A.Miagkov[41], M.Michelotto[35], E.Migliore[44], L.Mirabito[25], W.A.Mitaroff[49], U.Mjoernmark[24], T.Moa[43], R.Moeller[28], K.Moenig[9], M.R.Monge[13], P.Morettini[13], H.Mueller[17], K.Muenich[51], M.Mulders[30], L.M.Mundim[6], W.J.Murray[36], B.Muryn[14,18], G.Myatt[34], F.Naraghi[14], F.L.Navarria[5], S.Navas[48], K.Nawrocki[50], P.Negri[27], S.Nemecek[12], W.Neumann[51], N.Neumeister[49], R.Nicolaidou[3], B.S.Nielsen[28], M.Nieuwenhuizen[30], V.Nikolaenko[10], M.Nikolenko[10,16], P.Niss[43], A.Nomerotski[35], A.Normand[34], W.Oberschulte-Beckmann[17], V.Obraztsov[41], A.G.Olshevski[16], A.Onofre[21], R.Orava[15], G.Orazi[10], K.Osterberg[15], A.Ouraou[38], P.Paganini[19], M.Paganoni[9,27], P.Pages[10], R.Pain[23], H.Palka[18], Th.D.Papadopoulou[31], K.Papageorgiou[11], L.Pape[9], C.Parkes[34], F.Parodi[13], A.Passeri[39], M.Pegoraro[35], L.Peralta[21], H.Pernegger[49], M.Pernicka[49], A.Perrotta[5], C.Petridou[45], A.Petrolini[13], H.T.Phillips[36], G.Piana[13], F.Pierre[38], M.Pimenta[21], T.Podobnik[42], O.Podobrin[9], M.E.Pol[6], G.Polok[18], P.Poropat[45], V.Pozdniakov[16], P.Privitera[37], N.Pukhaeva[16], A.Pullia[27], D.Radojicic[34], S.Ragazzi[27], H.Rahmani[31], P.N.Ratoff[20], A.L.Read[32], M.Reale[51], P.Rebecchi[19], N.G.Redaelli[27], M.Regler[49], D.Reid[9], R.Reinhardt[51], P.B.Renton[34], L.K.Resvanis[3], F.Richard[19], J.Richardson[22], J.Ridky[12], G.Rinaudo[44], A.Romero[44], I.Roncagliolo[13], P.Ronchese[35], L.Roos[23], E.I.Rosenberg[1], P.Roudeau[19], T.Rovelli[5], W.Ruckstuhl[30], V.Ruhlmann-Kleider[38], A.Ruiz[40], K.Rybicki[18], H.Saarikko[15], Y.Sacquin[38], A.Sadovsky[16], O.Sahr[14], G.Sajot[14], J.Salt[48], M.Sannino[13], H.Schneider[17], U.Schwickerath[17], M.A.E.Schyns[51], G.Sciolla[44], F.Scuri[45], P.Seager[20], Y.Sedykh[16], A.M.Segar[34], A.Seitz[17], R.Sekulin[36], L.Serbelloni[37], R.C.Shellard[6], P.Siegrist[9,38], R.Silvestre[38], F.Simonetto[35], A.N.Sisakian[16], B.Sitar[7], T.B.Skaali[32], G.Smadja[25], N.Smirnov[41], O.Smirnova[24], G.R.Smith[36], R.Sosnowski[50], D.Souza-Santos[6], E.Spiriti[39], P.Sponholz[51], S.Squarcia[13], D.Stampfer[9], C.Stanescu[39], S.Stanic[42], S.Stapnes[32], I.Stavitski[35], K.Stevenson[34], A.Stocchi[19], J.Strauss[49], R.Strub[10], B.Stugu[4], M.Szczekowski[50], M.Szeptycka[50], T.Tabarelli[27], J.P.Tavernet[23], E.Tcherniaev[41], F.Tegenfeldt[47], F.Terranova[27], J.Thomas[34], A.Tilquin[26], J.Timmermans[30], L.G.Tkatchev[16], T.Todorov[10], S.Todorova[10], D.Z.Toet[30], A.Tomaradze[2], B.Tome[21], A.Tonazzo[27], L.Tortora[39], G.Transtromer[24], D.Treille[9], G.Tristram[8], A.Trombini[19], C.Troncon[27], A.Tsirou[9], M-L.Turluer[38], I.A.Tyapkin[16], M.Tyndel[36], S.Tzamarias[11], B.Ueberschaer[51], O.Ullaland[9], V.Uvarov[41], G.Valenti[5], E.Vallazza[45], G.W.Van Apeldoorn[30], P.Van Dam[30], J.Van Eldik[30], A.Van Lysebetten[2], N.Vassilopoulos[34], G.Vegni[27], L.Ventura[35], W.Venus[36], F.Verbeure[2], M.Verlato[35], L.S.Vertogradov[16], D.Vilanova[38], P.Vincent[25], L.Vitale[45], E.Vlasov[41], A.S.Vodopyanov[16], V.Vrba[12], H.Wahlen[51], C.Walck[43], F.Waldner[45], P.Weilhammer[9], C.Weiser[17], A.M.Wetherell[9], D.Wicke[51], J.H.Wickens[2], M.Wielers[17], G.R.Wilkinson[9], W.S.C.Williams[34], M.Winter[10], M.Witek[18], T.Wlodek[19], J.Yi[1], K.Yip[34], O.Yushchenko[41], F.Zach[25], A.Zaitsev[41], A.Zalewska[9], P.Zalewski[50], D.Zavrtanik[42], E.Zevgolatakos[11], N.I.Zimin[16], D.Zontar[42], G.C.Zucchelli[43], G.Zumerle[35]

[1] Department of Physics and Astronomy, Iowa State University, Ames IA 50011-3160, USA
[2] Physics Department, Univ. Instelling Antwerpen, Universiteitsplein 1, B-2610 Wilrijk, Belgium
and IIHE, ULB-VUB, Pleinlaan 2, B-1050 Brussels, Belgium
and Faculté des Sciences, Univ. de l'Etat Mons, Av. Maistriau 19, B-7000 Mons, Belgium
[3] Physics Laboratory, University of Athens, Solonos Str. 104, GR-10680 Athens, Greece
[4] Department of Physics, University of Bergen, Allégaten 55, N-5007 Bergen, Norway
[5] Dipartimento di Fisica, Università di Bologna and INFN, Via Irnerio 46, I-40126 Bologna, Italy
[6] Centro Brasileiro de Pesquisas Físicas, rua Xavier Sigaud 150, RJ-22290 Rio de Janeiro, Brazil
and Depto. de Física, Pont. Univ. Católica, C.P. 38071 RJ-22453 Rio de Janeiro, Brazil
and Inst. de Física, Univ. Estadual do Rio de Janeiro, rua São Francisco Xavier 524, Rio de Janeiro, Brazil
[7] Comenius University, Faculty of Mathematics and Physics, Mlynska Dolina, SK-84215 Bratislava, Slovakia
[8] Collège de France, Lab. de Physique Corpusculaire, IN2P3-CNRS, F-75231 Paris Cedex 05, France
[9] CERN, CH-1211 Geneva 23, Switzerland
[10] Centre de Recherche Nucléaire, IN2P3 - CNRS/ULP - BP20, F-67037 Strasbourg Cedex, France
[11] Institute of Nuclear Physics, N.C.S.R. Demokritos, P.O. Box 60228, GR-15310 Athens, Greece
[12] FZU, Inst. of Physics of the C.A.S. High Energy Physics Division, Na Slovance 2, 180 40, Praha 8, Czech Republic
[13] Dipartimento di Fisica, Università di Genova and INFN, Via Dodecaneso 33, I-16146 Genova, Italy
[14] Institut des Sciences Nucléaires, IN2P3-CNRS, Université de Grenoble 1, F-38026 Grenoble Cedex, France
[15] Helsinki Institute of Physics, HIP, P.O. Box 9, FIN-00014 Helsinki, Finland
[16] Joint Institute for Nuclear Research, Dubna, Head Post Office, P.O. Box 79, 101 000 Moscow, Russian Federation
[17] Institut für Experimentelle Kernphysik, Universität Karlsruhe, Postfach 6980, D-76128 Karlsruhe, Germany
[18] Institute of Nuclear Physics and University of Mining and Metalurgy, Ul. Kawiory 26a, PL-30055 Krakow, Poland
[19] Université de Paris-Sud, Lab. de l'Accélérateur Linéaire, IN2P3-CNRS, Bât. 200, F-91405 Orsay Cedex, France
[20] School of Physics and Chemistry, University of Lancaster, Lancaster LA1 4YB, UK
[21] LIP, IST, FCUL - Av. Elias Garcia, 14-1^o, P-1000 Lisboa Codex, Portugal
[22] Department of Physics, University of Liverpool, P.O. Box 147, Liverpool L69 3BX, UK
[23] LPNHE, IN2P3-CNRS, Universités Paris VI et VII, Tour 33 (RdC), 4 place Jussieu, F-75252 Paris Cedex 05, France
[24] Department of Physics, University of Lund, Sölvegatan 14, S-22363 Lund, Sweden
[25] Université Claude Bernard de Lyon, IPNL, IN2P3-CNRS, F-69622 Villeurbanne Cedex, France
[26] Univ. d'Aix - Marseille II - CPP, IN2P3-CNRS, F-13288 Marseille Cedex 09, France
[27] Dipartimento di Fisica, Università di Milano and INFN, Via Celoria 16, I-20133 Milan, Italy
[28] Niels Bohr Institute, Blegdamsvej 17, DK-2100 Copenhagen 0, Denmark
[29] NC, Nuclear Centre of MFF, Charles University, Areal MFF, V Holesovickach 2, 180 00, Praha 8, Czech Republic
[30] NIKHEF, Postbus 41882, NL-1009 DB Amsterdam, The Netherlands
[31] National Technical University, Physics Department, Zografou Campus, GR-15773 Athens, Greece
[32] Physics Department, University of Oslo, Blindern, N-1000 Oslo 3, Norway
[33] Dpto. Fisica, Univ. Oviedo, Avda. Calvo Sotelo, S/N-33007 Oviedo, Spain, (CICYT-AEN96-1681)
[34] Department of Physics, University of Oxford, Keble Road, Oxford OX1 3RH, UK
[35] Dipartimento di Fisica, Università di Padova and INFN, Via Marzolo 8, I-35131 Padua, Italy
[36] Rutherford Appleton Laboratory, Chilton, Didcot OX11 OQX, UK
[37] Dipartimento di Fisica, Università di Roma II and INFN, Tor Vergata, I-00173 Rome, Italy
[38] CEA, DAPNIA/Service de Physique des Particules, CE-Saclay, F-91191 Gif-sur-Yvette Cedex, France
[39] Istituto Superiore di Sanità, Ist. Naz. di Fisica Nucl. (INFN), Viale Regina Elena 299, I-00161 Rome, Italy
[40] Instituto de Fisica de Cantabria (CSIC-UC), Avda. los Castros, S/N-39006 Santander, Spain, (CICYT-AEN96-1681)
[41] Inst. for High Energy Physics, Serpukov P.O. Box 35, Protvino, (Moscow Region), Russian Federation
[42] J. Stefan Institute, Jamova 39, SI-1000 Ljubljana, Slovenia and Department of Astroparticle Physics, School of Environmental Sciences, Kostanjeviska 16a, Nova Gorica, SI-5000 Slovenia,
and Department of Physics, University of Ljubljana, SI-1000 Ljubljana, Slovenia
[43] Fysikum, Stockholm University, Box 6730, S-113 85 Stockholm, Sweden
[44] Dipartimento di Fisica Sperimentale, Università di Torino and INFN, Via P. Giuria 1, I-10125 Turin, Italy
[45] Dipartimento di Fisica, Università di Trieste and INFN, Via A. Valerio 2, I-34127 Trieste, Italy
and Istituto di Fisica, Università di Udine, I-33100 Udine, Italy
[46] Univ. Federal do Rio de Janeiro, C.P. 68528 Cidade Univ., Ilha do Fundão BR-21945-970 Rio de Janeiro, Brazil
[47] Department of Radiation Sciences, University of Uppsala, P.O. Box 535, S-751 21 Uppsala, Sweden
[48] IFIC, Valencia-CSIC, and D.F.A.M.N., U. de Valencia, Avda. Dr. Moliner 50, E-46100 Burjassot (Valencia), Spain
[49] Institut für Hochenergiephysik, Österr. Akad. d. Wissensch., Nikolsdorfergasse 18, A-1050 Vienna, Austria
[50] Inst. Nuclear Studies and University of Warsaw, Ul. Hoza 69, PL-00681 Warsaw, Poland
[51] Fachbereich Physik, University of Wuppertal, Postfach 100 127, D-42097 Wuppertal, Germany
[52] On leave of absence from IHEP Serpukhov

1 Introduction

Due to the small number of baryons (B) in hadronic Z^0 decays, the study of these particles offers the possibility of a more detailed understanding of the fragmentation processes than the study of mesons. Because baryons are produced only in pairs and at a relatively low rate, studies going beyond the simple comparison of the fragmentation properties of baryons and mesons can reveal finer details of the transition of partons into hadrons, e.g. how far the interactions in a string reach. In addition, the combined study of Λs and protons allows the compensation of strangeness to be studied.

Two available models that describe the formation of hadrons in e^+e^- annihilations are string and cluster fragmentation, which are implemented in the Monte Carlo programs JETSET [1] and HERWIG [2] respectively.

The string model describes the hadronization as several break-ups of a colour string, which is stretched between the partons (the colour-charged particles) that were produced in hard QCD processes. The string is a 1-dimensional object and has an energy density per unit length of $\kappa \approx 1$ GeV fm^{-1}. When the energy in the string becomes large enough, $q\overline{q}$ pairs are produced, breaking the string. The $q\overline{q}$ pairs are produced in a classically prohibited region and have to tunnel out into the allowed region. The probability of this process for quarks of mass m is proportional to $\exp(-\pi m^2/\kappa)$. However, as it is not clear whether the current algebra quark masses or the constituent quark masses should be used, the resulting suppression of $s\overline{s}$ production is left as a free parameter γ_s. The relative probabilities of creating $q\overline{q}$ pairs with different flavours are roughly $u\overline{u} : d\overline{d} : s\overline{s} : c\overline{c} = 1 : 1 : 0.3 : 10^{-11}$.

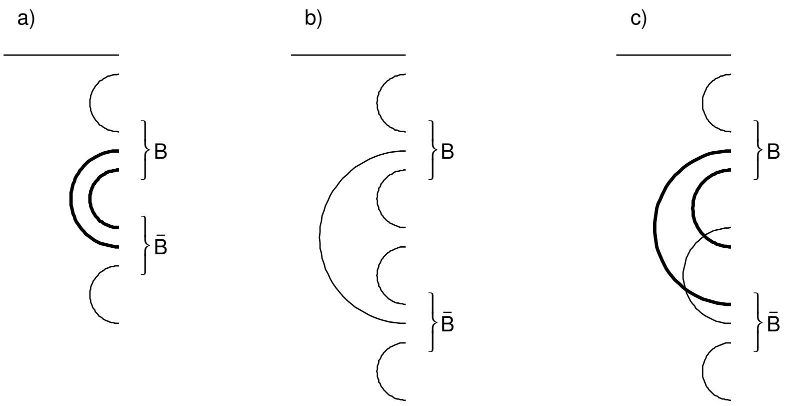

Figure 1: Schematic representation of the baryon production in the string model. The top lines indicate the primary quarks, and the semi-circles indicate quark-antiquark pairs that arise in the fragmentation.

Occasionally, the string can break up producing a diquark-antidiquark ($D\overline{D}$) pair. This process is very similar to producing a $q\overline{q}$ pair since both states, the $D\overline{D}$ and the $q\overline{q}$, are pairs of colour triplets and colour anti-triplets. With the neighbouring quark and antiquark in the string, the $D\overline{D}$ pair will form a baryon-antibaryon pair (Fig. 1 a). This *direct* process is controlled by parameters that describe

- the relative probability of producing a diquark-antidiquark pair $q_1q_2\overline{q_1q_2}$ rather than a $q\overline{q}$ pair, P_{qq},
- the additional suppression of diquarks that contain an $s\overline{s}$ pair over diquarks that consist only of u and d quarks, δ_s, leading to an overall suppression of $P_{qq} \cdot \gamma_s \cdot \delta_s$ for diquarks with one strange quark, and
- the suppression of spin 1 over spin 0 diquarks, P_1.

Baryons can also be formed when $q\overline{q}$ pairs overlap in other ways. This mechanism is called *popcorn* [3], and is illustrated in Figs. 1 b) and c). Figure 1 b) focuses more on the fact that in the popcorn model the quarks are in principle produced separately, while Fig. 1 c) underlines more the close relationship with, and possible transition to, the direct diquark fragmentation in Fig. 1 a). The rapidity is defined as $y = \frac{1}{2}\ln\frac{E+p_{\parallel}}{E-p_{\parallel}}$, where E is the energy of the particle and $p_{\parallel}$ the projection of the momentum onto the thrust axis. Neighbouring baryons in the string typically differ in rapidity by about 1, with popcorn fragmentation leading to bigger rapidity differences than the direct process. Thus the rapidity correlation of baryon-antibaryon pairs is a tool to study the popcorn mechanism, i.e. to study to what extent baryons are locally produced. The fraction f of baryons that are produced via the popcorn mechanism, and the additional suppression of strange quarks inside a popcorn quark configuration, are determined by three further free parameters [†].

Previous publications on baryon production stated either that the data on $\Lambda\overline{\Lambda}$ rapidity correlations [5–7] and on $p\overline{p}$ rapidity correlations [8] are in agreement with a relative probability of popcorn production of 0.5, or that the data indicate larger values. However, a difficulty in distinguishing direct baryon production from popcorn production is the fact that the particles produced in the fragmentation subsequently decay. If either or both of two baryons, originally produced directly as neighbours in the string (Fig. 1a), are unstable and decay before they are detected, the resulting particle configuration can be very similar to that arising when stable hadrons are produced via popcorn fragmentation. In a similar way, the decay products of mesons with large decay energies can overlap the rapidity range of a directly produced baryon pair. The fraction f should therefore only be determined in an overall tuning of the generator to the measured data.

In the cluster model as implemented in Herwig, there is only one production mode for baryons. According to the available phase space, depending on the masses of the clusters and the produced hadrons, clusters can decay into one or two mesons or a baryon-antibaryon pair. There are no free parameters to control this process. Since Herwig produces a higher rate of baryons with very short lifetimes than Jetset, decays play a bigger role.

2 Event and particle selections

A general description of the Delphi detector and its performance can be found in references [9] and [10]. Features of the apparatus relevant for the analysis of multi-hadronic final states (with emphasis on the detection of charged particles) are outlined in reference [11].

In this analysis, hadronic events were selected using the standard criteria as defined in reference [10]. The analysis is based on $2.74 \cdot 10^6$ multihadronic events recorded in the years 1992 through 1994.

The biases in the analysis due to the detector acceptance and performance and the selection criteria were studied and corrected using the full detector simulation program Delsim [10]. Around 10^7 events were generated using the Jetset 7.3 PS model with parameters tuned as in reference [12]. The particles were followed through the detailed detector geometry, and simulated data were produced and processed by the same analysis program as the real data.

[†]A revised version of the popcorn model, in which the stepwise production of the quarks is carried through consistently and the number of free parameters is reduced, has recently been developed [4], but is not yet generally available.

2.1 Selection of Λ Baryons

The DELPHI procedure for reconstructing neutral 2-body decays (V^0) is described in [10]. Candidate decays are found by considering all pairs of oppositely charged particles. The vertex defined by each pair is determined by minimising the χ^2 obtained from the distances from the vertex to the extrapolated tracks. V^0 candidates flagged as 'standard' or 'tight' by this package are considered as Λ candidates, if they fulfil the following additional criteria:

1. the radii in the x-y plane ‡ of the first measured points of the two outgoing tracks are not *both* more than 5 cm smaller than the radius of the secondary vertex R_{vtx};
2. the radial separation R_{flight} of the primary vertex and the secondary vertex in the x-y plane is greater than 10 times the error on the fitted distance;
3. the angle $\Delta\varphi$ in the x-y plane between the V^0 momentum and the line joining the primary to the fitted secondary vertex is less than 0.01 rad;
4. at least one of the outgoing tracks has a χ^2 probability from the track fit of more than 10^{-5};
5. the secondary vertex lies well inside the tracking system: $R_{\mathrm{vtx}} < 75$ cm and $|z_{\mathrm{vtx}}| < 70$ cm;
6. the mass pull (the absolute mass shift from the nominal mass divided by its error) is smaller with respect to the Λ mass than with respect to the K^0 mass.

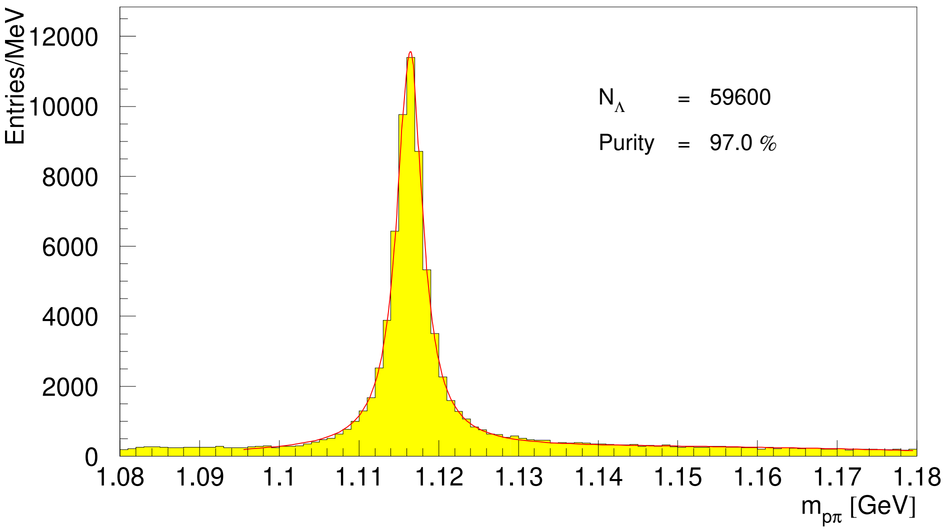

Figure 2: Invariant mass distribution of reconstructed Λ candidates. The quantities N_Λ and purity refer to a mass window of $1.108\,\mathrm{GeV} < m_{p\pi} < 1.124\,\mathrm{GeV}$ and are obtained from a fit of the sum of a Breit-Wigner function and a second order polynomial to the mass distribution.

Criteria 1–3 enrich the sample with genuine Λs that originate from the primary vertex. Criteria 4–5 slightly improve the mass resolution by rejecting badly measured Λ decays. Criterion 6 suppresses the K^0 background. If two candidates share a track, the one whose reconstructed mass is closer to the Λ mass is used. A set of 69200 Λ-Baryons is selected with a purity of 90.7 %.

‡The z axis of the cartesian coordinate system is along the positron beam.

To reduce the background further, candidates for which the outgoing particle with the higher momentum is identified as a pion by the measurement of the Cherenkov angle in the RICH (see below), or for which both candidates are identified as electrons, are rejected. The pion rejection exploits the fact that there are only very few charged kaons among the tracks in the background candidates. The mass distribution of the 59600 Λ-Baryons selected from the 1994 data set is shown in Fig. 2. In order to achieve similar angular acceptances for Λ baryons and protons the polar angle, θ, has to be additionally restricted to the barrel region (47° to 133°).

2.2 Selection of Charged Hadrons

The DELPHI detector contains Ring Imaging CHerenkov (RICH) detectors to perform pion, kaon and proton identification [10]. The barrel RICH detector [13] consists of a liquid (C_6F_{14}) radiator and a gaseous (C_5F_{12}) radiator, combined with a detector sensitive to single Cherenkov photons. Both radiators are operational for Cherenkov angle measurement of particles with momenta from 0.7 up to 45 GeV.

In this analysis, pion, kaon and proton tagging was performed using the NEWTAG package [14]. This is based on the RIBMEAN clustering algorithm which reconstructs a weighted mean Cherenkov angle [10]. NEWTAG is optimised for different combinations of liquid and gas radiator information in different momentum windows between 0.7 and 45 GeV. For each hypothesis, a 'loose', 'standard' or 'tight' tag output is given by NEWTAG, which basically correspond to the tagged particle being within 2.5 standard deviations of the hypothesis and separated by more than 1, 2 or 3 standard deviations respectively from the nearest neighbour hypothesis. NEWTAG also gives a track by track tag-quality output, based on the combined RIBMEAN liquid and gas quality flags.

For momenta below 1.3 GeV, down to 0.3 GeV, tagging can be performed based on the measurement of the specific ionisation, $\mathrm{d}E/\mathrm{d}x$, in the DELPHI Time Projection Chamber (TPC) [10]: a particle is tagged if its $\mathrm{d}E/\mathrm{d}x$ is measured to be within 1.5 standard deviations of the hypothesis.

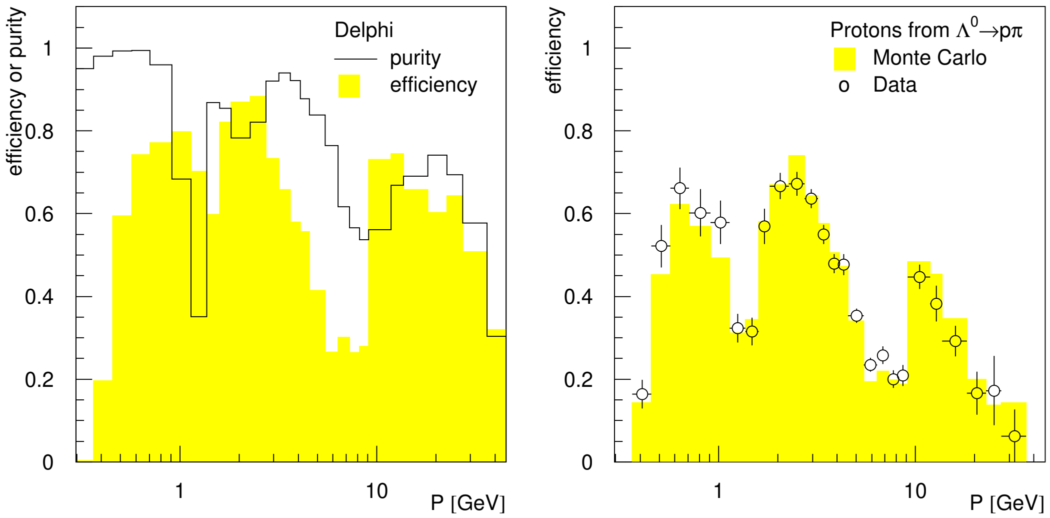

Figure 3: Left: Proton tag efficiency (shaded histogram) and purity (line) within the angular acceptance of the Outer Detector versus momentum. Right: Proton tag efficiency for protons from Λ-decay in data and simulation.

For this analysis, the selection of charged particles was restricted to a momentum window from 0.3 GeV to 45 GeV in the barrel region of DELPHI (polar angles between

47° and 133°), and the barrel RICH was required to be fully operational. For momenta above 0.7 GeV, only those particles were used for which at least the Outer Detector[§] and the TPC information were used for the track reconstruction. Below 0.7 GeV, all particles which had at least 50 wire hits in the TPC were used.

To achieve an optimal balance between proton tagging efficiency and purity, the momentum window from 0.3 GeV to 45 GeV was divided into six different tag windows. From 0.3 to 0.7 GeV the TPC $\mathrm{d}E/\mathrm{d}x$ tag was required, while from 0.7 to 1.3 GeV the tight NEWTAG tag was required in addition. From 1.3 to 3 GeV and from 9 to 11.5 GeV, only the loose NEWTAG tag was required, and from 3 to 9 GeV and from 11.5 to 45 GeV, only the standard one. The impact parameter was required to be smaller than 1.5 cm in the R-φ-plane and smaller than 3 cm in z.

Fig. 3 shows on the left hand side the efficiency (light shaded histogram) of the proton tag and the purity (line) of the tagged proton sample as a function of momentum, derived from 1994 full detector simulation. Giving the momentum bins between 0.3 and 45 GeV equal weight, the mean efficiency is 56.4% and the mean purity is 75.8%. In the TPC, low momentum particles yield large ionisation signals which saturate the electronics, causing the proton tagging efficiency to be very small below 0.4 GeV.

The right hand side of Fig. 3 shows the agreement in efficiency between data and simulation for tagging protons in a subsample of 'tight' Λ candidates from the DELPHI V^0 reconstruction [10]. The impact parameter was required to be smaller than 10 cm in the R-φ-plane and smaller than 20 cm in z. The difference in efficiency between the left and right hand sides of Fig. 3 is due to the fact that the proton purity of the Λ candidate subsample is only 64.6% (giving equal weight to each bin). After the proton tagging, this purity rises to 96.3%.

3 Baryon Correlations

3.1 Rapidity Difference

The analysis of $\Lambda\Lambda$ pairs used the data taken from 1992 through 1994, which comprise $2.74 \cdot 10^6$ hadronic events. For proton identification over the entire momentum range, both the liquid and the gas radiator of the RICH detector need to be operational. Therefore the analysis of Λp and pp pairs was restricted to the data taken in 1994 ($1.33 \cdot 10^6$ hadronic events).

The protons and Λ baryons were selected as described in section 2. Hadronic events with

$$N_{\mathrm{B}} = N_{\mathrm{p}} + N_{\Lambda} = 2 \quad , \tag{1}$$

were selected (Table 1), where N_{p}, N_{Λ} are the numbers of protons and Λs respectively (antibaryons are included). Events with more than two baryons were excluded, because already in the case of $N_{\mathrm{B}} = 3$ at least two of the three possible combinations are uncorrelated. When selecting the baryons, double counting was avoided by requiring that the Λs did not share a common outgoing track, and that the protons were not part of a reconstructed Λ. To obtain a purer sample of direct protons, the Λ selection used for this veto criterion was less restrictive and was 50 % more efficient. This reduced the fraction of tagged protons originating from Λ decays from 7 % to 5 %, as estimated from the simulation.

[§]The Outer Detector is situated radially beyond the barrel RICH.

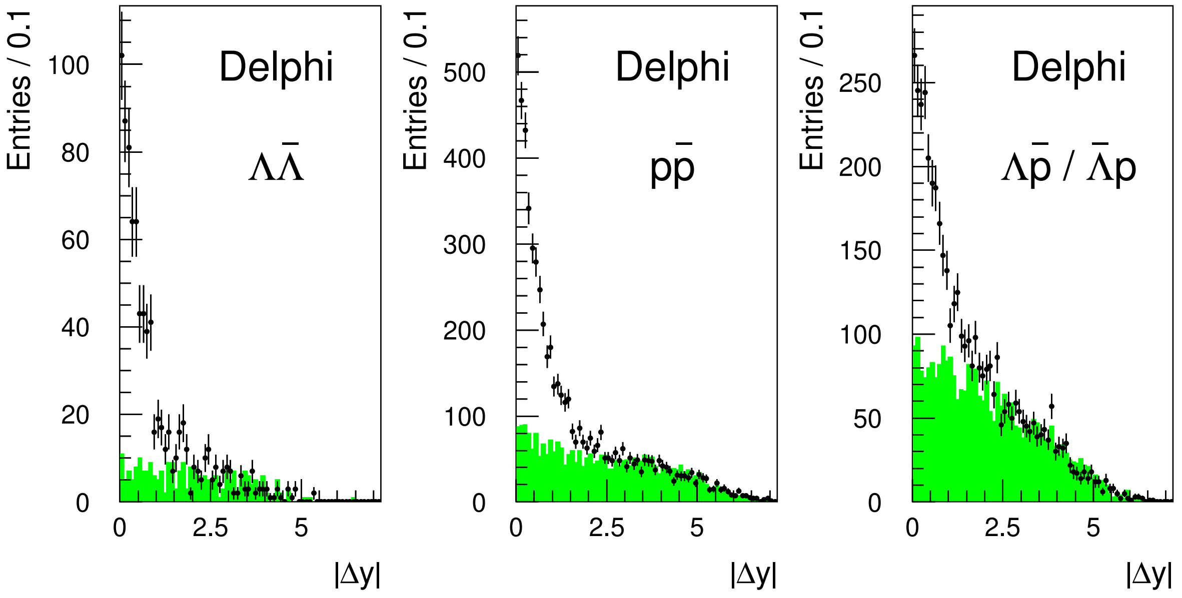

Figure 4: Rapidity differences of baryon-antibaryon pairs (points with error bars) compared to those of baryon-baryon and antibaryon-antibaryon pairs (shaded histograms) from DELPHI data.

Figure 4 shows the differences in rapidity with respect to the thrust axis of the event for the three different types of baryon pairs. The pairs with non-zero baryon number, shown shaded, consist of different sources of background. The analysis-specific background is due to misidentifications (of one or both of the baryons) and inefficiencies (e.g. only a Λp pair of a $\Lambda\bar{\Lambda}$-p$\bar{\text{p}}$ event is reconstructed). But even with an ideal reconstruction and identification, one would find uncorrelated baryon pairs from events with more than one baryon pair, because of baryons that are not included in the analysis (e.g. n and Σ).

3.2 Background Subtraction

To determine the rapidity difference distribution for correlated B$\overline{\text{B}}$ pairs, the background as estimated from the sum of the distributions of the BB and the $\overline{\text{BB}}$ pairs was subtracted. Statistical fluctuations of the background distributions were reduced by fitting a third order polynomial spline function before the subtraction.

The subtracted rapidity difference distributions have to be corrected for additional detector acceptance effects, like the limitation to the barrel region. These tend to strengthen the correlation observed. The correction factors were obtained from the full simulation and were found to have a linear behaviour in $|\Delta y|$. Consequently the corrections were carried out using the result of a straight line fit to the correction function. The pairs of fit parameters for the three different B$\overline{\text{B}}$ types agreed within their statistical errors. Thus a common correction factor calculated from the mean values of the three parameter pairs could be used, independently of the B$\overline{\text{B}}$ type.

Figure 5 compares the resulting rapidity difference distributions both in data and in full simulation. There are only very few pairs with absolute differences greater than 2. Thus correlated baryons are always either both in a common jet or both in the inter-jet region. There is no evidence for a long range baryon correlation.

Combination	$n(\mathrm{B\overline{B}})$	$n(\mathrm{BB}) + n(\mathrm{\overline{BB}})$	$n(\mathrm{B\overline{B}}) - n(\mathrm{\overline{BB}}) - n(\mathrm{BB})$	$\frac{(n(\mathrm{\overline{BB}}) + n(\mathrm{BB}))}{n(\mathrm{B\overline{B}})}$
pp	5552	2764	2788	48.8 %
ΛΛ	772	225	547	29.1 %
	1829	602	1227	32.9 %
Λp	2922	1519	1403	52.0 %

Table 1: Numbers of pairs for the different baryon combinations. The second line for ΛΛ contains the numbers for all data sets from 1992 through 1994, whereas the other lines refer only to the data taken in 1994.

	$\frac{1}{n_{\mathrm{pair}}} \left\langle \frac{\mathrm{d}n}{\mathrm{d}\Delta y} \right\rangle \Big\|_{\|\Delta y\|<0.2}$	
Baryon pair	Real Data	Simulation
$\mathrm{p\bar{p}}$	1.05 ± 0.06	1.10 ± 0.03
$\Lambda\bar{\Lambda}$	1.14 ± 0.08	1.17 ± 0.05
$\Lambda\mathrm{\bar{p}},\ \bar{\Lambda}\mathrm{p}$	0.77 ± 0.08	1.10 ± 0.05

Table 2: Comparison of peak heights (see Fig. 5) for real data and JETSET 7.3 full simulation. The errors are statistical only.

While pairs of baryons of the same type are highly correlated, and show a similar behaviour for $\Lambda\overline{\Lambda}$ and $\mathrm{p\overline{p}}$ pairs, the mixed pairs are clearly less correlated and exhibit a plateau in the range $|\Delta y| < 0.4$. This suggests that the popcorn probability might be higher for the mixed pairs. This is discussed further below. The three points with error bars on the upper right hand side of each part of Fig. 5 show the mean of the two leftmost bins ($|y(\mathrm{B}) - y(\overline{\mathrm{B}})| < 0.2$) for the three $\mathrm{B\overline{B}}$ combinations. The values of these peak heights are compared in Table 2.

3.3 Systematic Effects

Several checks of the stability and significance of the observed difference in the rapidity correlation were carried out. For Λs and protons, two different selections were used. Charged particle identification was omitted in the Λ selection, which lowered the purity from 97.0 % to 90.7 %. The influence of protons from hadronic interactions and other secondary decays was investigated by relaxing the requirements on the impact parameters of the proton tracks. By checking the stability of the signal over the data taking period between 1992 and 1994, detector dependent fluctuations were excluded. This also checked the effects of Λ reconstruction with or without the aid of the z coordinate readout of the

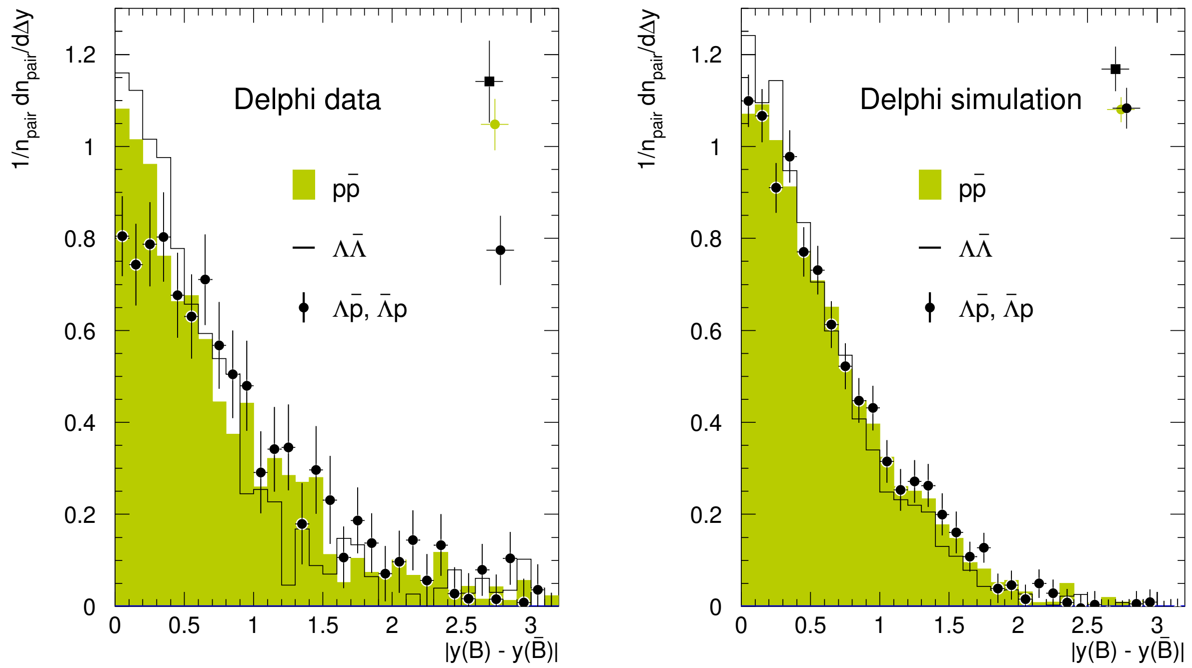

Figure 5: Rapidity differences of baryon-antibaryon pairs for real data and full JETSET 7.3 simulation with DELPHI tuning [12]. The three points with error bars on the far right of each plot show the mean values of the two leftmost bins ($|y(\mathrm{B}) - y(\overline{\mathrm{B}})| < 0.2$), referred to as peak heights in Table 2, for the three $\mathrm{B}\overline{\mathrm{B}}$ combinations, to show the significance of the effect.

silicon vertex detector[¶]. The shapes of the background distributions, as obtained from the BB and the $\overline{\mathrm{BB}}$ pairs, were compared with those based on a) background candidates taken from the sidebands of the Λ mass distribution and b) randomly selected charged particles instead of tagged protons. This was done for BB- and $\overline{\mathrm{BB}}$-like pairs as well as for $\mathrm{B}\overline{\mathrm{B}}$-like pairs. None of those changes significantly affected the rapidity correlations. This indicates that systematic uncertainties can be neglected, so only statistical errors are quoted.

Finally, it should perhaps be remarked that not only do $\simeq 5\%$ of the tagged protons come from Λ decays, as remarked earlier, but some others originate from $\Sigma^{\pm}$ and a similarly small fraction of the Λ are from $\Xi^{\pm,0}$ decays, etc. However, all these effects are included in the simulation, and at about the same level as in the real data, so they are not expected to explain the effect observed.

3.4 Total Pair Numbers

Besides the rapidity correlation, the relative production rates of different $\mathrm{B}\overline{\mathrm{B}}$ pairs depend on details of the production mechanism, such as the fraction from the popcorn

[¶]Until 1993 the vertex detector consisted of three layers of single sided silicon strip detectors at average radii R = 6.3, 9.0, and 10.9cm providing only an R-Φ measurement in the plane transverse to the beam. In 1994, two layers were upgraded with double sided readout including also the z coordinate. At the same time the DELPHI V^0 reconstruction procedure was updated to take advantage of the higher z resolution.

mechanism in the JETSET model. The quantity

$$q = \frac{N(\Lambda\mathrm{p})}{\sqrt{N(\Lambda\Lambda)N(\mathrm{pp})}} \quad , \tag{2}$$

with $N(\mathrm{B_1B_2}) = n(\mathrm{B_1}\overline{\mathrm{B_2}}) + n(\overline{\mathrm{B_1}}\mathrm{B_2}) - n(\overline{\mathrm{B_1B_2}}) - n(\mathrm{B_1B_2})$ and $\mathrm{B_1}$, $\mathrm{B_2} = \Lambda$ or p, allows a comparison of the pair production rates on a basis largely independent of detector acceptance. Whereas the JETSET simulation gives $q_{\mathrm{sim}} = 1.03 \pm 0.03$, the real data give $q_{\mathrm{data}} = 1.10 \pm 0.04$. Since the pair rates are not statistically independent if the pairs are selected requiring $N_{\mathrm{B}} = 2$, the values for q were determined once more including all possible pair combinations in events with $N_{\mathrm{B}} = 3$ or 4. Then the simulation value remains the same, while the data yield a slightly lower value of $q_{\mathrm{data}} = 1.08 \pm 0.04$.

The distribution of the rapidity difference did not change when the pairs in events with $N_{\mathrm{B}} = 3$ or 4 were used.

3.5 Comparison to the Fragmentation Models

In the JETSET 7.3 full simulation, which was generated with a popcorn fraction $f = 0.5$, the three types of $\mathrm{B\overline{B}}$ combination give rise to similar rapidity difference distributions (see right hand plot in Fig. 5). The HERWIG generator also predicts only small differences between the peak heights of the three $\mathrm{B\overline{B}}$ combinations. Here we consider whether these predictions are intrinsic properties of the two models, or only of the two particular generators and their tunings.

In the string model as implemented in the JETSET version 7.3, the baryons are created via direct diquark fragmentation in $1-f$ of the cases while in the other cases the popcorn model is used. The different flavour composition modes as given in Table 3 would lead to different relative weights of popcorn production for the various baryon combinations.

$\mathrm{B\overline{B}}$ Pair	direct diquark		popcorn fragmentation	
	diquarks	relative probability	common quarks	relative probability
pp	ud, uu	$2+1$	u, d	$2+1$
$\Lambda\Lambda$	ud, us, ds	$2{\gamma_{\mathrm{s}}}^2+4\gamma_{\mathrm{s}}\delta_{\mathrm{s}}$	u, d, s	$2{\gamma_{\mathrm{s}}}^2(1+\delta_{\mathrm{s}}+\sqrt{\delta_{\mathrm{s}}})+2\gamma_{\mathrm{s}}\delta_{\mathrm{s}}$
Λp	ud	$2\gamma_{\mathrm{s}}$	u, d	$2\gamma_{\mathrm{s}}+2\gamma_{\mathrm{s}}\sqrt{\delta_{\mathrm{s}}}$

Table 3: Possible flavour configurations in JETSET. The right column contains the relative suppression of the popcorn fragmentation for the $\Lambda\Lambda$ case and the relative enhancement for the Λp case according to their flavour composition modes.

The relative probabilities of the various modes as given in the table are fully determined by the inner quarks along the string, i.e. by those $\mathrm{q\overline{q}}$ pairs which contribute only to the $\mathrm{B\overline{B}}$ system, or to the $\mathrm{BM\overline{B}}$ system in the case of popcorn fragmentation. If one of the inner quarks is an s in only one baryon, the suppression factor is $\sqrt{\delta_{\mathrm{s}}}$ instead of δ_{s}. For popcorn fragmentation leading to a Λp configuration, only one quark is shared among the two baryons, and can be u or d. Thus there are more production modes than for direct diquark fragmentation, where two quarks are shared. This would tend to make the relative probability of popcorn fragmentation bigger for the mixed pairs, as the data suggest. Nevertheless, the correlations in JETSET are almost independent of the $B\overline{B}$ type.

There are other relevant suppression factors besides γ_s and δ_s that are not taken into account in Table 3. For example, the branching into different flavour modes is also influenced by the fraction of spin 1 diquarks, because when a $D\overline{D}$ pair consists of two $q\overline{q}$ pairs of the same flavour, it has to have spin 1 to allow the overall baryon wave function to be antisymmetric. The change of the spin 3/2 baryon rate following an altered spin 1 diquark suppression would give rise to a conflict with data, but this consequence could be avoided by using another free parameter in JETSET, `PARJ(18)`, which allows an extra suppression of spin 3/2 baryons and is 1 by default (no suppression). However, it has been tested that with a spin 1 diquark suppression, P_1, decreased by a factor A (i.e. with `PARJ(4)`$= 0.07 \cdot A$, where 0.07 is the value in the DELPHI tuning), and accordingly with `PARJ(18)`$= 1/A$, for $A = 3$ and 14 the simulated correlations do not change substantially.

Since baryons in HERWIG can only be produced as pairs in cluster decays, they are always highly correlated, regardless and independently of the $B\overline{B}$ combination. The small differences in the correlations (the peak heights differ by at most 0.04) can only arise from the hadron decays after the fragmentation. Less correlated pairs and correlations which depend on the $B\overline{B}$ combination could be described by introducing three body cluster decays, for which similar considerations apply as to the popcorn model. Cluster decays into more than two particles are already implemented in the program CALTECH II [15], in which a small string is stretched to describe the decay of massive clusters.

Thus, by correctly handling the different flavour modes to give different relative weight to the popcorn fragmentation in JETSET, and by including three body cluster decays in the cluster model, there would be scope to modify the model implementations to reproduce the observed rapidity distributions for the three analysed types of baryon pair. Hence these results are not necessarily in contradiction with the principles of the string or cluster fragmentation models, but just with the implementations of these models by the Monte Carlo programs.

3.6 Mesons in the Rapidity Window

The Λp pairs offer the possibility to check the correlation of the baryon pairs with mesons having a rapidity between those of the two baryons. If exactly one meson is found in the rapidity window, one might naturally expect it to be a kaon more often for the Λp pairs than for $\Lambda\Lambda$ or pp, to compensate for the strangeness difference between the baryons.

$B\overline{B}$ pairs with $\Delta y = |y(\mathrm{B}) - y(\overline{\mathrm{B}})|$ below 1.0 are considered as potentially correlated and the BB pairs with Δy below 1.0 as measuring their uncorrelated background. Table 4 gives the fractions of correlated pairs where exactly one pion or one kaon is found in the rapidity gap between the two baryons.

No enrichment of kaons inside Λp pairs is found. Also, the strangeness of the kaon matches that of the Λ ($\Lambda K^+\overline{p}$ or $\overline{\Lambda}K^-p$) as often as not. Hence the correlation seen between the baryons is not strictly extended to the mesons in the rapidity gap between the two baryons. This is consistent with the hypothesis that the decays of unstable particles smear the correspondence between the rapidity and the rank in the string.

	Real Data		JETSET 7.3 Full Simulation	
$B\overline{B}$ Pair	fraction of $B\overline{B}$ pairs with		fraction of $B\overline{B}$ pairs with	
	one pion	one kaon	one pion	one kaon
$p\overline{p}$	0.25 ± 0.02	0.07 ± 0.01	0.25 ± 0.01	0.07 ± 0.01
$\Lambda\overline{\Lambda}$	0.26 ± 0.03	0.07 ± 0.01	0.24 ± 0.01	0.07 ± 0.01
$\Lambda\overline{p}$	0.26 ± 0.02	0.05 ± 0.01	0.25 ± 0.01	0.06 ± 0.01

Table 4: Fractions of $B\overline{B}$ pairs with kaons and pions in the rapidity gap between the two baryons for real data and the JETSET 7.3 full simulation. The backgrounds estimated from pairs with non-zero baryon number have been subtracted. The numbers are not corrected for detector acceptance.

3.7 Rapidity Difference with Respect to the Charged Kaons

Λp events in which exactly one charged kaon is found, regardless of its rapidity, offer a further possibility to analyse how far the rapidity correlation that has been found in the baryon pairs applies also for the mesons in the vicinity.

The Λp pairs are split into three samples: correlated pairs with a small rapidity difference, $|\Delta y_B| < 0.6$, pairs with a bigger difference, $0.6 < |\Delta y_B| < 2$, and mostly uncorrelated pairs with $2 < |\Delta y_B|$. Only pairs with opposite baryon numbers are taken into account: the events where strangeness is not compensated (ΛK^- and $\overline{\Lambda}K^+$, $S = \pm 2$) are assumed to describe the background of misidentified and uncorrelated events with accidentally compensated strangeness (ΛK^+ and $\overline{\Lambda}K^-$, $S = 0$). Thus the distributions of the $S = \pm 2$ pairs are subtracted from the ones with compensated strangeness. The ratio of the number of $S = \pm 2$ pairs to the number of $S = 0$ pairs is $(72 \pm 5)\%$ in real data and $(68 \pm 2)\%$ in the simulation. The purity of correctly identified particle trios in the simulation is about 50 % in the case $|\Delta y_B| < 0.6$, and about 40 % in the case $0.6 < |\Delta y_B| < 2$.

No correlation with respect to the kaon is visible if $2 < |\Delta y_B|$. For $|\Delta y_B| < 2$ the correlation with respect to the kaon follows the correlation between the baryons (Fig. 6). A high correlation between the baryons is associated with a high correlation between the kaon and the Λ. The link between the two correlations is also present in the JETSET simulation, but it seems to be smaller.

4 Summary

Rapidity difference distributions for protons and Λ baryons have been presented and compared with JETSET and HERWIG simulations. The rapidity correlations for $\Lambda\overline{\Lambda}$ and $p\overline{p}$ pairs agree with each other and with the JETSET model expectation. The correlation for $\Lambda\overline{p}$ pairs is smaller than for $\Lambda\overline{\Lambda}$ or $p\overline{p}$ pairs. This effect is described neither by JETSET nor by HERWIG, although it is not necessarily in disagreement with the principles of the string or cluster fragmentation models.

Particle decays after the fragmentation process could play an important role in smearing the rapidity spectrum. This is indicated by the fact that the mesons in the rapidity gap between neighbouring baryons do not show a dependence on the baryon combination.

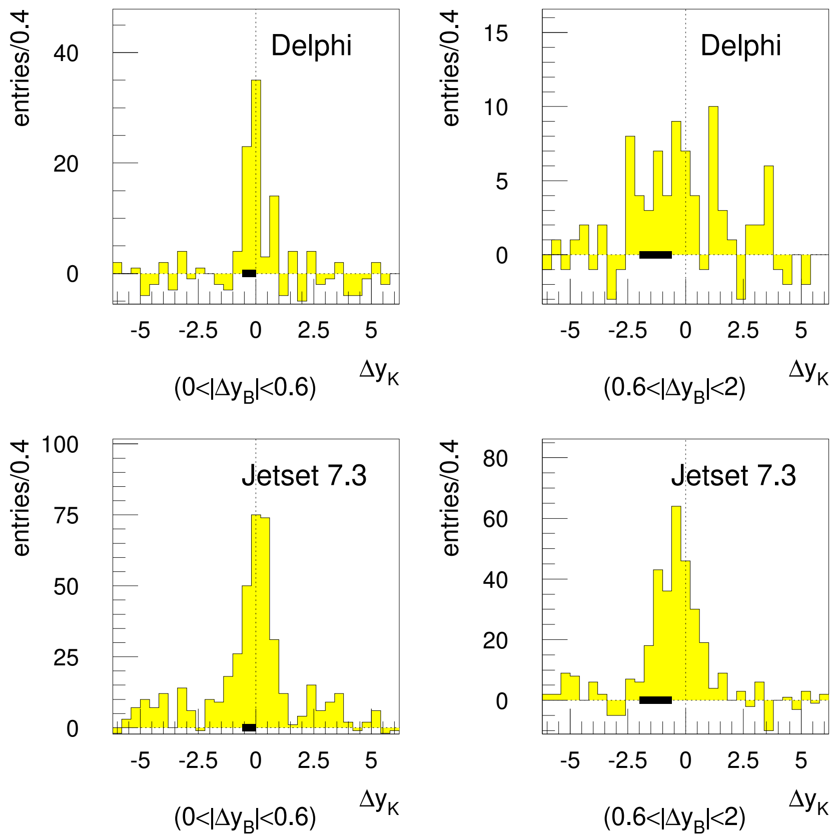

Figure 6: Rapidity difference $y_K - y_\Lambda$ between the kaon and the Λ for two ranges of the rapidity difference of the Λp pair. The two upper plots are obtained from the data and the two lower ones from the DELSIM simulation, which contains 3.5 times more events than the data. The sign of y is chosen such that $\Delta y_B = y_p - y_\Lambda$ would be negative. The position range of Δy_B is indicated as a black bar on the abscissa.

For $\Lambda\overline{p}$ pairs, there is evidence for a short range compensation of strangeness depending on the rapidity difference of the baryon pair. The behaviour is qualitatively described by the JETSET simulation.

Acknowledgements

We would like to thank Patrik Eden (University of Lund) and Mike Seymour (CERN) for discussing and explaining the consequences for the Monte Carlo generators. We are greatly indebted to our technical collaborators and to the funding agencies for their support in building and operating the DELPHI detector, and to the members of the CERN-SL Division for the excellent performance of the LEP collider.

References

[1] T. Sjöstrand, *Computer Physics Communications* **82** (1994) 74.

[2] G. Marchesini, et al., *Computer Physics Communications* **67** (1992) 465.

[3] A. Casher, H. Neuberger, and S. Nussinov, *Phys. Rev.* **D20** (1979) 179;
B. Andersson, G. Gustafson, and T. Sjöstrand, *Physica Scripta* **32** (1985) 574.

[4] P. Eden, G. Gustafson, *Baryon Production in the String Fragmentation Picture*, LU-TP 96-20, hep-ph/9606454.

[5] Opal Collaboration, P.D. Acton, et al., *Phys. Lett.* **B305** (1993) 415.

[6] Delphi Collaboration, P. Abreu et al., *Phys. Lett.* **B318** (1993) 249.

[7] Aleph Collaboration, D. Buskulic et al., *Z. Phys.* **C64** (1994) 361.

[8] Aleph Collaboration, *Proton-Antiproton Correlations in Hadronic Z Decays*, Contributed paper eps0422 to the Int. Europhysics Conf. on High Energy Physics, Brussels, Belgium, July 1995.

[9] Delphi Collaboration, P. Aarnio et al., *Nucl. Instr. and Meth.* **A303** (1991) 233.

[10] Delphi Collaboration, P. Abreu et al., *Nucl. Instr. and Meth.* **A378** (1996) 57.

[11] Delphi Collaboration, P. Aarnio et al., *Phys. Lett.* **B240** (1990) 271.

[12] Delphi Collaboration, P. Abreu et al., *Z. Phys.* **C73** (1996) 11.

[13] E.G. Anassontzis et al., *Nucl. Instr. and Meth.* **A323** (1992) 351;
W. Adam et al., *Nucl. Instr. and Meth.* **A343** (1994) 68;
W. Adam et al., *Nucl. Instr. and Meth.* **A338** (1994) 284;
Delphi rich Collaboration, contributions to the Second Workshop on rich Detectors, Uppsala 1995, *Nucl. Instr. and Meth.* **A371** (1996).

[14] E. Schyns, newtag — *π, K, p Tagging for* Delphi rich*es*, Delphi Note 96-103 RICH 89.

[15] T.D. Gottschalk, D.A. Morris, *Nucl. Phys.* **B288** (1987) 729;
D.A. Morris, Ph.D. Thesis, CALT-68-1440 (1987).